Eur. Phys. J. C 29, 549–556 (2003)
Digital Object Identifier (DOI) 10.1140/epjc/s2003-01228-y

THE EUROPEAN PHYSICAL JOURNAL C

Hadron resonance mass spectrum and lattice QCD thermodynamics*

F. Karsch[1], K. Redlich[1,2], A. Tawfik[1]

[1] Fakultät für Physik, Universität Bielefeld, Postfach 100 131, 33501 Bielefeld, Germany
[2] Institute of Theoretical Physics, University of Wroclaw, 50204 Wroclaw, Poland

Received: 16 April 2003 /
Published online: 8 July 2003 –

Abstract. We confront lattice QCD results on the transition from the hadronic phase to the quark–gluon plasma with hadron resonance gas and percolation models. We argue that for $T \leq T_c$ the equation of state derived from Monte Carlo simulations of $(2+1)$ quark-flavor QCD can be well described by a hadron resonance gas. We examine the quark mass dependence of the hadron spectrum on the lattice and discuss its description in terms of the MIT bag model. This is used to formulate a resonance gas model for arbitrary quark masses which can be compared to lattice calculations. We finally apply this model to the analysis of the quark mass dependence of the critical temperature obtained in lattice calculations. We show that the value of T_c for different quark masses agrees with lines of constant energy density in a hadron resonance gas. For large quark masses a corresponding contribution from a glueball resonance gas is required.

1 Introduction

Long before lattice calculations provided first evidence [1] for critical behavior in strongly interacting matter it has been noticed [2] by Hagedorn that ordinary hadronic matter cannot persist as a hadronic resonance gas at arbitrary high temperatures and densities. This lead to the concept of the Hagedorn limiting temperature. With the formulation of QCD it has been suggested [3] that a phase transition to a new form of matter, the quark–gluon plasma, will occur.

Two basic properties of hadrons were essential for developing the concept of a natural end for the era of ordinary hot and dense hadronic matter. In high energy experiments it had been observed that strongly interacting particles produce a large number of new resonances. Moreover, hadrons have been known to be extended particles with a typical size of about 1 fm. As the average energy per particle increases at high temperatures copious particle production will take place in a hadron gas and a dense equilibrated system will result from this. At high temperature, extended hadrons thus would start to "overlap". This led to the expectation that some form of new physics has to occur under such conditions. The expected critical behavior has been analyzed in terms of various phenomenological models which incorporate these basic features (resonance production ⇒ Hagedorn's bootstrap model [2]; extended hadrons ⇒ percolation models [4]). In fact, many of the basic properties of the dense matter created today in heavy ion experiments can be understood quite well in terms of the thermodynamics of a hadronic resonance gas [5,6].

With the formulation of quantum chromodynamics (QCD) as a theoretical framework for the strong interaction force among elementary particles it became clear that this "new physics" indeed meant a phase transition to a new phase of strongly interacting matter – the quark–gluon plasma (QGP) [3]. As QCD is an asymptotically free theory, the interaction vanishes logarithmically with increasing temperature; it has been expected that at least at very high temperatures the QGP would effectively behave like an ideal gas of quarks and gluons. Today we have a lot of information from numerical calculations within the framework of lattice regularized QCD about the thermodynamics of hot and dense matter which give support to these expectations. We know about the transition temperature to the QGP and the temperature dependence of basic bulk thermodynamic observables such as the energy density and the pressure [7]. In the coming years the increase in numerical accuracy certainly will lead to modifications of the quantitative details of these results. However, already today they are sufficiently accurate to be confronted with theoretical and phenomenological models that provide a description of thermodynamics of strongly interacting matter. Recently, progress has been made to develop and link an improved perturbation theory of QCD with lattice data on the equation of state in the deconfined phase [8]. In this paper we analyze in how far the critical behavior can be understood in terms of the physical degrees of freedom of the confined phase, i.e. those of a hadronic resonance gas, and the intuitive percolation picture [9].

* Dedicated to Rolf Hagedorn

Quite distinct from the phenomenological approaches to the QCD phase transition are attempts to understand the thermodynamics of strongly interacting matter in terms of low energy effective theories, i.e. chiral perturbation theory [10] and effective chiral models [11,12]. The strength of these approaches is that they incorporate the correct symmetries of the QCD Lagrangian and thus have a chance to predict the universal properties, e.g. the order of the phase transition, in the chiral limit of QCD. They, however, generally ignore the contributions of heavier resonances to the QCD thermodynamics which might be crucial for the transition to the plasma phase at non-vanishing values of the quark masses.

Lattice calculations provide detailed information on the quark mass dependence of the transition to the QGP as well as to the hadron spectrum at zero temperature. In particular, we know that the transition temperature drops substantially when decreasing the quark mass from infinity (pure $SU(3)$ gauge theory) to values close to the physical quark mass. This drop in the critical temperature can be understood at least qualitatively in terms of the relevant degrees of freedom in the low temperature phase. In the pure gauge limit this phase consists of rather heavy glueballs ($m_G \gtrsim 1.5\,\mathrm{GeV}$ [13–15]). Quite a large temperature thus is needed to build up a sufficiently large density of glueballs, which could lead to critical behavior (percolation [9]). In the chiral limit, on the other hand, the low critical temperature can be addressed in the presence of light Goldstone particles, the pions, which can build up a large (energy) density already at rather low temperatures. Along with this decrease of the critical temperature goes an increase in the critical energy density expressed in units of the critical temperature, ϵ_c/T_c^4, by about an order of magnitude. This reflects the importance of new degrees of freedom in the presence of light quarks. However, at the same time the critical energy density in physical units ($\mathrm{GeV/fm^3}$) turns out to be almost quark mass independent.

In this paper we want to focus on these results. We will discuss in how far the quark mass dependence of the transition temperature found in lattice calculations is consistent with phenomenological models and what this tells us about the influence of the chiral sector of QCD on the transition temperature. In Sect. 2 we will briefly summarize the formulation of hadron thermodynamics in terms of a hadronic resonance gas. In Sect. 3 we discuss the quark mass dependence of the hadron spectrum and give a phenomenological parametrization motivated by the bag model. Predictions of these phenomenological approaches for the equation of state and the quark mass dependence of the transition temperature are then compared with lattice results in Sect. 4. Finally we give our conclusions in Sect. 5.

2 Hadron resonance gas and the equation of state on the lattice

The basic quantity required to verify thermodynamic properties of QCD is the partition function[1] $Z(T,V)$. The grand canonical partition function is obtained by

$$Z(T,V) = \mathrm{Tr}[\mathrm{e}^{-\beta H}], \tag{1}$$

where H is the Hamiltonian of the system and $\beta = 1/T$ is the inverse temperature. The confined phase of QCD we model as a non-interacting gas of resonances – the hadron resonance gas model. To do so we use as Hamiltonian the sum of kinetic energies of relativistic Fermi and Bose particles of mass m_i.

The main motivation of using this Hamiltonian is that it contains all relevant degrees of freedom of the confined, strongly interacting matter and implicitly includes interactions that result in resonance formation [2]. In addition this model was shown to provide a quite satisfactory description of particle production in heavy ion collisions [5, 6, 16].

With the above assumption on the dynamics the partition function can be calculated exactly and expressed as a sum over one-particle partition functions Z_i^1 of all hadrons and resonances,

$$\ln Z(T,V) = \sum_i \ln Z_i^1(T,V). \tag{2}$$

For particles of mass m_i and spin–isospin degeneracy factor g_i the one-particle partition function Z_i^1 is given by

$$\ln Z_i^1(T,V) = \frac{V g_i}{2\pi^2} \int_0^\infty \mathrm{d}p p^2 \eta \ln(1 + \eta \mathrm{e}^{-\beta E_i}), \tag{3}$$

where $E_i = \sqrt{p^2 + m_i^2}$ is the particle energy and $\eta = -1$ for bosons and $+1$ for fermions.

Due to the factorization of the partition function in (2) the energy density and the pressure of the hadron resonance gas,

$$\epsilon = \sum_i \epsilon_i^1, \; P = \sum_i P_i^1, \tag{4}$$

are also expressed as sums over single particle contributions ϵ_i^1 and P_i^1, respectively. These are given by

$$\frac{\epsilon_i^1}{T^4} = \frac{g_i}{2\pi^2} \sum_{k=1}^{\infty} (-\eta)^{k+1} \frac{(\beta m_i)^3}{k} \times \left[\frac{3\, K_2(k\beta m_i)}{k\beta m_i} + K_1(k\beta m_i) \right], \tag{5}$$

$$\Delta_i^1 \equiv \frac{\epsilon_i^1 - 3P_i^1}{T^4} = \frac{g_i}{2\pi^2} \sum_{k=1}^{\infty} (-\eta)^{k+1} \frac{(\beta m_i)^3}{k} K_1(k\,\beta m_i), \tag{6}$$

where K_1 and K_2 are modified Bessel functions.

Summing up in (4) the contributions from experimentally known hadronic states constitutes the resonance gas model for the thermodynamics of the low temperature

[1] We restrict our discussion to the case of vanishing chemical potential (vanishing net baryon number) and charge neutral systems

phase of QCD. We take into account all mesonic and baryonic resonances with masses up to 1.8 GeV and 2.0 GeV, respectively. This amounts to 1026 resonances. The energy density obtained in the resonance gas starts to rise rapidly at a temperature of about 160 MeV. It reaches a value of 0.3 GeV/fm^3 at $T \simeq 155$ MeV and 1 GeV/fm^3 already at $T \simeq 180$ MeV. This is in good agreement with lattice calculations, which find [17] a critical energy density of about 0.7 GeV/fm^3 at $T_c \simeq 170$ MeV. For comparison we note that a simple pion gas would only lead to an energy density of about 0.1 GeV/fm^3 at this temperature. This suggests that a more quantitative comparison between numerical results obtained from lattice calculations and the resonance gas model might indeed be meaningful.

3 Hadron spectrum in heavy quark mass limit

In order to use the resonance gas model for further comparison with lattice results we should take into account that lattice calculations are generally performed with quark masses heavier than those realized in nature. In fact, we should take advantage of this by comparing lattice results obtained for different quark masses with resonance gas model calculations based on a modified, quark mass dependent, resonance spectrum.

Rather than converting the bare quark masses used in lattice calculation into a renormalized mass it is much more convenient to use directly the pion mass ($m_\pi \sim \sqrt{m_q}$), i.e. the mass of the Goldstone particle, as a control parameter for the quark mass dependence of the hadron spectrum.

For our thermodynamic considerations we need, at present, not be concerned with the detailed structure of the hadron spectrum in the light quark mass chiral limit. We rather want to extract information on the gross features of the quark mass dependence of a large set of resonances. In order to study the quark mass dependence of hadron masses in the intermediate region between the chiral and heavy quark mass limits we adopt here an approach that is based on the Hamiltonian of the MIT bag model [18]. Although, in the original formulation this Hamiltonian breaks explicitly chiral symmetry and implies non-conservation of the axial-vector current it still provides a satisfactory description of the hadron mass spectrum that can be used for our thermodynamic considerations.

In the limit of a static, spherical cavity the energy of the bag of radius R is given by

$$E = E_V + E_0 + E_K + E_M + E_E. \tag{7}$$

The first two terms are due to quantum fluctuations and are assumed to depend only on the bag radius. The volume and the zero-point energy terms have a generic form

$$E_V = \frac{4}{3}\pi B R^3, \quad E_0 = -\frac{Z_0}{R}, \tag{8}$$

where B is the bag constant and Z_0 is a phenomenological parameter attributed to the surface energy.

The quarks inside the bag contribute with their kinetic and rest energy. Assuming N quarks of mass m_i the quark kinetic energy is determined from

$$E_K = \frac{1}{R}\sum_{i=1}^{N}[x_i^2 + (m_i R)^2]^{1/2}, \tag{9}$$

where $x_i(m_i, R)$ enters the expression on the frequency $\omega = [x^2 + (mR)^2]^{1/2}/R$ of the lowest quark mode and is obtained [18] as the smallest positive root of the following equation:

$$\tan(x_i) = \frac{x_i}{1 - m_i R - \sqrt{x_i^2 + (m_i R)^2}}. \tag{10}$$

The last two terms in (7) represent the color-magnetic and -electric interaction of quarks. It is described by the exchange of a single gluon between two quarks inside the bag. The color-electric energy was found in [18] to be numerical small and will be neglected in our further discussion. The color-magnetic exchange term is given by

$$E_M = 8k\alpha_c \sum_{i<j} \frac{M(m_i R, m_j R)}{R}(\sigma_i \cdot \sigma_j). \tag{11}$$

Here α_c is the strong coupling constant and $k = 1$ for baryons and 2 for mesons. For a given spin configuration of the bag the scalar spin product in (11) can easily be calculated. The function $M(x, y)$ depends on the quark modes magnetic moment and is described in detail in [18]. For small $x < 1$ it shows a linear dependence on the argument with $M(0, 0) = 0.175$.

The dependence of the energy on the bag radius can be eliminated by the condition that the quark and gluon field pressure balance the external vacuum pressure. For a static spherical bag this condition is equivalent to minimizing E with respect to R. The true radius R_0 of the bag thus is determined from the condition $\partial E/\partial R = 0$ and the hadron bag mass is then obtained from (7) with $R = R_0$.

To extract the physical mass spectrum from the MIT bag model one still needs to fix the set of five parameters that determine the bag energy. Following the original fit to experimental data made in [18] we take $B^{1/4} = 0.145$ GeV, $Z_o = 1.84$ and $\alpha_c = 0.55$. These parameters together with $m_u = m_d = 0$ and $m_s = 0.279$ GeV provide a quite satisfactory description of hadron masses belonging to the octet and decuplet of baryons and the octet of vector mesons. Of course, the model fails to describe the details of the chiral limit and, in particular, it leads to a too large value of the pion mass that with the above set of parameters is $m_\pi = 0.28$ GeV. Nonetheless, the accuracy of the bag model will be sufficient for our purpose.

The MIT bag model provides an explicit dependence of hadron masses on the constituent quark mass. This dependence is entirely determined by the kinetic and magnetic energy of the quarks. To compare bag model calculations with lattice calculations, which do not provide values for constituent quark masses, it is best to express the quark

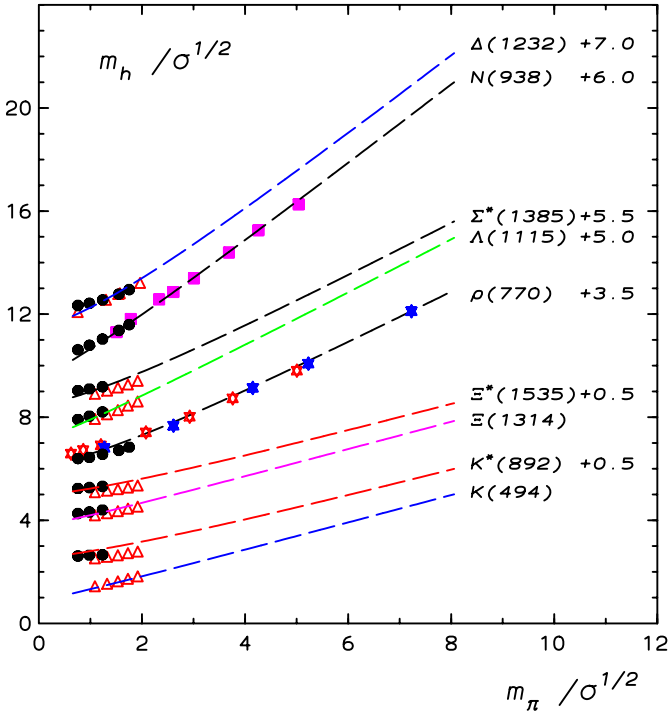

Fig. 1. Dependence of different hadron masses m_h on the pion mass m_π. Both m_h and m_π are expressed in the units of the string tension $\sqrt{\sigma}$. Curves are the MIT bag model results (see text for details). The filled circles represent the PC-PACS lattice results from [23]. The filled diamonds are the $N_f = 3$, whereas the open diamonds are $N_f = 2$ flavor results from [22]. The filled-boxes are quenched QCD results [24]. All other points are from [25]. Both the lattice data and the bag model results are shifted in m_h-direction by a constant factor as indicated in the figure

mass dependence in terms of the pion mass, which is most sensitive to changes of the quark masses. In Fig. 1 we show the resulting dependence of different hadron masses on the pion mass with the bag parameters described above but with varying m_u. The masses are expressed in units of the square root of the string tension for which we use $\sqrt{\sigma} = 420\,\mathrm{MeV}$.

The model predictions are compared with recent lattice data on hadron masses calculated for different current quark masses [22–25]. The MIT bag model is seen in Fig. 1 to describe lattice results quite well. This is particularly the case for larger quark masses such that $m_\pi > \sqrt{\sigma}$. For $m_\pi < \sqrt{\sigma}$ the deviations of the model from the lattice results are quite apparent. As mentioned this is, of course, mainly due to the well known limitations of the bag model when approaching the chiral limit.

For large quark masses the bag model description of hadron masses reproduces the naive parton model picture and consequently all hadron masses are almost linearly increasing with the pion mass as seen in Fig. 1. This is to be expected as in this case the energy of the bag is entirely determined by the quark rest mass. As seen in Fig. 1 the slope increases with the number of non-strange constituent quarks inside the bag. Consequently, the slopes

Table 1. Parameters entering the interpolation formula for non-strange hadron masses given in (12)

a_1	a_2	a_3	a_4	a_5
0.51 ± 0.1	$\frac{a_1 N_u}{m_0}$	0.115 ± 0.02	-0.0223 ± 0.008	0.0028 ± 0.0015

of (Ξ^*, Ξ) and (K, K^*) or (Σ^*, Λ) and ρ coincide at large m_π.

In order to formulate a resonance gas model for arbitrary quark masses we need to know the quark mass dependence of much more resonances than the few hadronic states shown in Fig. 1. We thus looked for a phenomenological parameterization of the quark mass dependence of resonances, expressed in terms of the pion mass. Figure 1 suggests that already at intermediate values of the quark mass, $m_\pi \gtrsim \sqrt{\sigma}$, this dependence is dominated by the quark rest mass and does not depend much on the hadronic quantum numbers. This suggests that a common parameterization of all hadronic states, which is consistent with the naive parton model picture for large quark masses and reproduces the experimental values of hadronic states in the light quark mass limit, is sufficient for our thermodynamic considerations. To incorporate these features we use the ansatz

$$\frac{M(x)}{\sqrt{\sigma}} \simeq N_u a_1 x + \frac{m_0}{1 + a_2 x + a_3 x^2 + a_4 x^3 + a_5 x^4}, \quad (12)$$

which provides a good description of the MIT bag model result for non-strange hadron masses calculated for different values of m_π. Here $x \equiv m_\pi/\sqrt{\sigma}$, $m_0 \equiv m_\mathrm{h}/\sqrt{\sigma}$, N_u is the number of light quarks inside the hadron ($N_u = 2$ for mesons, $N_u = 3$ for baryons) and $\sigma = (0.42\,\mathrm{GeV})^2$ is the string tension.

The parameters appearing in (12) were optimized such that they reproduce the MIT bag model results for the m_π-dependence of the ρ vector meson mass and are summarized in Table 1. In the mass regime shown in Fig. 1, (12) reproduces the quark mass dependence of all non-strange hadron masses obtained from the bag model within a relative error of $\lesssim 6\%$.

In the following we will use (12) to formulate a hadron resonance gas model with varying quark masses and compare its predictions with the lattice calculation of QCD thermodynamics.

In Fig. 2 we show the temperature dependence of the energy density ϵ and the interaction measure Δ for the hadron resonance gas obtained from (4)–(6) and (12). The model predictions are compared with Monte Carlo results obtained [17] on the lattice in (2+1) flavor QCD. Although it should be noted that the lattice calculations have not yet been performed with the correct quark mass spectrum realized in nature, as the pion mass $m_\pi \sim 1.8\sqrt{\sigma}$, the resonance gas model and the lattice data agree quite well. This indicates that for $T \leq T_\mathrm{c}$ hadronic resonances are indeed the most important degrees of freedom in the confined phase.

In the next section we will discuss in how far this model can provide a quantitative description of the transition

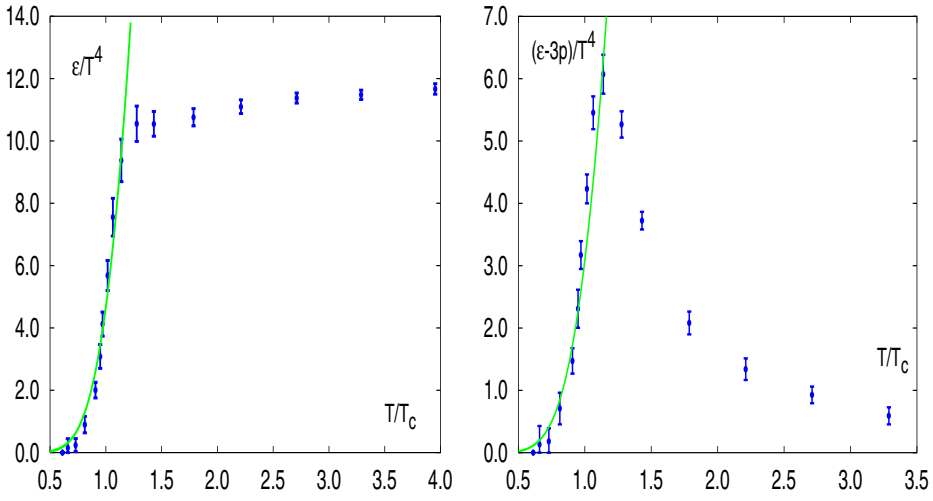

Fig. 2. The left-hand figure shows the energy density ϵ in units of T^4 calculated on the lattice with $(2+1)$ quark flavors as a function of the T/T_c ratio. The right-hand figure represents the corresponding results for the interaction measure $(\epsilon - 3P)/T^4$. The full lines are the results of the hadron resonance gas model that accounts for all mesonic and baryonic resonances

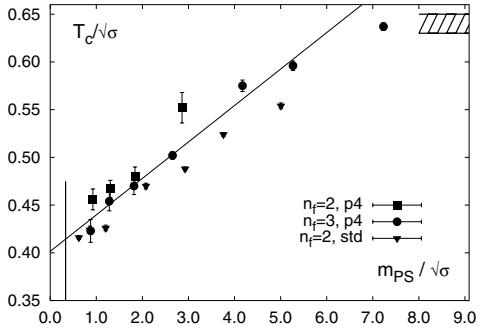

Fig. 3. The transition temperature in 2- (filled squares) and 3- (circles) flavor QCD versus $m_{\rm PS}/\sqrt{\sigma}$ using an improved staggered fermion action (p4-action). Also shown are results for 2-flavor QCD obtained with the standard staggered fermion action (open squares). The dashed band indicates the uncertainty on $T_c/\sqrt{\sigma}$ in the quenched limit. The straight line is the fit given in (13)

temperature obtained on the lattice for different quark masses.

4 Quark mass dependence of the QCD transition

We want to confront here the resonance gas model developed in the previous section with lattice results on the quark mass dependence of the QCD transition temperature and use it to learn about the critical conditions near deconfinement. Lattice calculations suggest that this transition is a true phase transition only in small quark mass intervals in the light and heavy quark mass regime, respectively. In a broad intermediate regime, in which the pion mass changes by more than an order of magnitude, the transition is not related to any singular behavior of the QCD partition function. Nonetheless, it still is well localized and is characterized by rapid changes of thermodynamic quantities in a narrow temperature interval. The transition temperature thus is well defined and is determined in lattice calculations through the location of maxima in response functions such as the chiral susceptibility. A collection of transition temperatures obtained in calculations with 2 and 3 quark flavors with degenerate masses is shown in Fig. 3. The main feature of the numerical results which we want to explore here is that the transition temperature varies rather slowly with the quark mass. In [17] the almost linear behavior has been described by the fit

$$\left(\frac{T_c}{\sqrt{\sigma}}\right)_{m_{\rm PS}/\sqrt{\sigma}} = 0.4 + 0.04(1)\,\left(\frac{m_{\rm PS}}{\sqrt{\sigma}}\right), \qquad (13)$$

which also is shown in Fig. 3. For pion masses $m_{\rm PS} \sim (6\text{–}7)\sqrt{\sigma} \simeq 2.5\,{\rm GeV}$ the transition temperature reaches the pure gauge value, $T_c/\sqrt{\sigma} \simeq 0.632(2)$ [27].

We note that all numerical results shown in Fig. 3 do correspond to quark mass values in the crossover regime. Also the resonance gas model formulated in the previous section does not lead to a true phase transition. We thus may ask what the conditions in a hadron gas are that trigger the transition to the plasma phase. Using the hadron gas with a quark mass dependent hadron mass spectrum and including the same set of 1026 resonances which have been included in other phenomenological calculations [5, 6] we have constructed resonance gas models for 2- and 3-flavor QCD, respectively. In the former case we eliminate all states containing strange quarks whereas in the latter case we assigned to meson states containing strange particles the corresponding masses of non-strange particles, e.g. kaons have been replaced by pions etc. With these resonance gas models we have calculated the energy density at the transition temperature. We use $T_c = 175\ (15)$ MeV for 2-flavor QCD and $T_c = 155\ (15)$ MeV for 3-flavor QCD, respectively. For the energy densities at the transition point

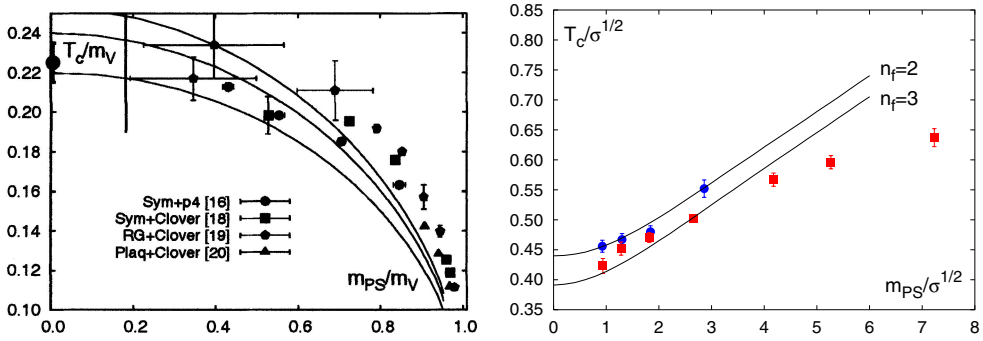

Fig. 4. The transition temperature versus pion mass obtained in lattice calculations and lines of constant energy density calculated in a resonance gas model. The left-hand figure shows a comparison of constant energy density lines at 1.2 (upper), 0.8 (middle) and 0.4 (lower) GeV/fm^3 with lattice results for 2-flavor QCD obtained with improved staggered [17] as well as improved Wilson [19–21] fermion formulations. T_c as well as m_{PS} are expressed in terms of the corresponding vector meson mass. The right-hand figure shows results for 2- and 3-flavor QCD compared to lines of constant energy density of 0.8 GeV/fm^3. Here T_c and m_{PS} are expressed in units of $\sqrt{\sigma}$. For a detailed description see text

we then find

$$\left(\frac{\epsilon}{T^4}\right)_{T=T_c} \simeq \begin{cases} 4.5 \pm 1.5, & \text{2-flavor,} \\ 7.5 \pm 2, & \text{3-flavor.} \end{cases} \qquad (14)$$

This is in good agreement with the lattice result, $\epsilon/T_c^4 = (6 \pm 2)$ quoted in [28] as an average for the 2- and 3-flavor energy densities. In fact, as can be seen from Fig. 5 in [28] the difference in ϵ/T_c^4 in the lattice results is of similar magnitude as we found here from the resonance gas model. The lattice results for 2- and 3-flavor QCD thus suggest that the conditions at the transition point are well described by a resonance gas. For comparison we also note that in the 2-flavor case a pion gas does contribute only about 20% to this energy density[2] and also a gas build up from the 20 lowest resonances would give rise only to about half the critical energy density, i.e. $\epsilon/T_c^4 \simeq 1.9$.

Although the lattice results allow, at present, only to determine the critical energy density within a factor (2–3) it is striking that the transition occurs at similar values of the energy density in QCD with light quarks as well as in the pure gauge theory, although the transition temperature shifts by about 40% and ϵ/T_c^4 differs by an order of magnitude. It thus has been suggested that for arbitrary quark masses the transition occurs at roughly constant energy density. Such an assumption is, in fact, supported by our resonance gas model constructed in the previous section for arbitrary values of the quark masses. In Fig. 4 we show lines of constant energy density calculated in the resonance gas model and compare these to the transition temperatures obtained in lattice calculations. As can be seen, the agreement is quite good up to masses $m_{PS} \simeq 3\sqrt{\sigma}$ or $m_{PS} \simeq 1.2$ GeV. The reason for the deviations at larger values of the quark mass, of course, is the fact that we have neglected so far completely the glueball sector in our considerations.

When the lightest hadron mass becomes comparable to typical glueball masses, also the glueball sector will start to contribute a significant fraction to the energy density.

[2] For massless pions we have $\epsilon/T^4 = (n_f^2 - 1)\pi^2/30 \simeq 1$

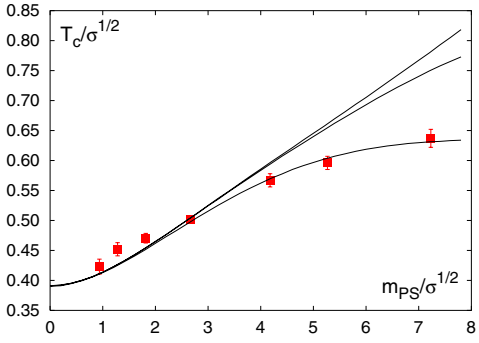

Fig. 5. The transition temperature in 3-flavor QCD compared to lines of constant energy density ($\epsilon = 0.8$ GeV/fm^3) in a hadronic resonance gas (upper curve), a hadronic resonance gas with 15 glueball states added (middle curve) and a hadronic resonance gas with 15 glueball states with a 40% reduced mass (lower curve)

Using the set of 15 different glueball states so far identified in lattice calculations [13] we have calculated their contribution to the total energy density. At $m_{PS}/\sqrt{\sigma} \simeq 6.5$ they contribute as much as the entire hadronic sector.

However, as can be seen in Fig. 5 the contribution of these 15 states only leads to a small shift in the lines of constant energy density. Similar to the hadronic resonance gas for small quark masses where the 20 low-lying states only contribute 50% of the total energy density one has to expect that also in the large quark mass limit further glueball states, which have so far not been identified, will contribute to the thermodynamics. Further support for this comes from a calculation of the energy density of the 15 known glueball states at the transition temperature of the pure gauge theory, $T = 0.63\sqrt{\sigma}$. For this we obtain $\epsilon(T = 0.63\sqrt{\sigma}) \simeq= .06$ GeV/fm^3 or equivalently $\epsilon/T_c^4 \simeq 0.1$, which is about 20% of the overall energy density at T_c.

The contribution of the 15 glueball states thus does not seem to be sufficient. In fact, the transition temperature in d-dimensional $SU(N_c)$ gauge theories is well understood in terms of the critical temperature of string models,

$T_c/\sqrt{\sigma} = \sqrt{3/\pi(d-2)}$, which also is due to an exponentially rising "mass" spectrum for string excitations [29].

It is conceivable that extending the glueball mass spectrum to all higher excited states will improve the results shown in Fig. 5. On the other hand one also should stress that the glueball states used in our calculations were obtained in quenched QCD and at zero temperature. There are indications from lattice calculations that glueball masses could be modified substantially in the presence of dynamical quarks [15] as well as at finite temperature [14]. The analysis of glueball states at high temperature [14] suggests that their masses can drop by $\sim$ (20–40)%. As all glueballs are heavy on the temperature scale of interest, shifts in their masses influence the thermodynamics much more strongly than in the light quark mass regime where the lowest state has already a mass which is of the order of the transition temperature. In fact, we find that taking into account a possible decrease of the glueball masses close to T_c seems to be more important than adding further heavy states to the spectrum. We thus have included a possible reduction of glueball masses in the equation of state. The resulting T_c with this modification is also shown in Fig. 5. Decreasing the glueball masses increases the thermal phase space available for particles, thus consequently the temperature required to get $\epsilon = 0.8\,\mathrm{GeV/fm^3}$ is decreasing. As can be seen in Fig. 5 a reduction of glueball masses by 40% is sufficient to reproduce lattice results in the whole m_π range. However, to make this comparison more precise it clearly would be important to get a more detailed understanding of the glueball sector.

5 Conclusions

In this paper we have analyzed lattice results on QCD thermodynamics using a phenomenological hadron resonance gas model. We have shown that close to the chiral limit and for $T \leq T_c$ the equation of state derived on the lattice is quantitatively well described by the resonance gas.

The hadron resonance gas partition function is also shown to be suitable to describe lattice results for finite quark masses and a varying number of flavors. One needs, however, to implement the quark mass dependence in the hadron spectrum and for large values of the quark mass the glueball degrees of freedom start to play an important role. We have shown that, beyond the chiral limit, the quark mass dependence arising from the MIT bag model agrees quite well with the hadron mass spectrum calculated on the lattice. We find that the transition temperatures obtained in lattice calculations at different values of the quark mass are well described by lines of constant energy density in a resonance gas model. For moderate values of the quark masses the predictions of the hadron resonance model coincide with lattice calculations. However, for heavy quark masses this agreement could only be achieved by including additional heavy glueball states or allowing for a reduction of glueball masses close to the transition temperature by about 40%.

Our results can be considered as an indication that the thermodynamics in the vicinity of deconfinement is indeed driven by the higher excited hadronic states. This finding can give additional support for previous phenomenological applications of the resonance gas partition function in the description of particle production in heavy ion collisions. Our discussion of the critical temperature and its quark mass dependence also indicates that deconfinement in QCD to a large extent is density driven. It would be interesting to see to what extent the lines of constant energy density of the generalized hadron resonance gas can be related to correspondingly generalized percolation models.

Acknowledgements. We acknowledge stimulating discussions with R. Baier, P. Braun-Munzinger, E. Laermann, D. Miller, J. Stachel and H. Satz. K.R. also acknowledges the support of the Alexander von Humboldt Foundation (AvH). This work has partly been supported by the DFG under grant FOR 339/2-1.

References

1. L.D. McLerran, B. Svetitsky, Phys. Lett. B **98**, 195 (1981); J. Kuti, J. Polonyi, K. Szlachanyi, Phys. Lett. B **98**, 199 (1981); J. Engels, F. Karsch, I. Montvay, H. Satz, Phys. Lett. B **101**, 89 (1981)
2. R. Hagedorn, Nuovo Cimento **35**, 395 (1965); R. Hagedorn, Thermodynamics of strong interactions, CERN Report 71-12 (1971)
3. N. Cabibbo, G. Parisi, Phys. Lett. B **59**, 67 (1975)
4. G. Baym, Physica A **96**, 131 (1979); T. Celik, F. Karsch, H. Satz, Phys. Lett. B **97**, 128 (1980)
5. P. Braun-Munzinger, D. Magestro, K. Redlich, J. Stachel, Phys. Lett. B **518**, 41 (2001); J. Cleymans, K. Redlich, Phys. Rev. C **60**, 054908 (1999); Phys. Rev. Lett. 81 (1998) 5284; F. Becattini et al., Phys. Rev. C **64**, 024901 (2001)
6. For a recent review see for instance: P. Braun-Munzinger, K. Redlich, J. Stachel, Particle Production in Heavy Ion Collisions, to appear in Quark Gluon Plasma 3, edited by R. Hwa, X.-N. Wang
7. F. Karsch, Lect. Notes. Phys. **583**, 202 (2002)
8. F. Karsch, A. Patkos, P. Petreczky, Phys. Lett. B **401**, 69 (1997); J.P. Blaizot, E. Iancu, A. Rebhan, Phys. Rev. Lett. **83**, 2906 (1999); R. Baier, K. Redlich, Phys. Rev. Lett. **84**, 2100 (2000); J.O. Andersen, E. Braaten, M. Strickland, Phys. Rev. D **61**, 074016 (2000)
9. H. Satz, Nucl. Phys. A **642**, 130 (1998)
10. P. Gerber, H. Leutwyler, Nucl. Phys. B **321**, 387 (1989)
11. H. Meyer-Ortmanns, B.-J. Schaefer, Phys. Rev. D **53**, 6586 (1996)
12. J. Berges, D. U. Jungnickel, C. Wetterich, Phys. Rev. D **59**, 034010 (1999)
13. C. Michael, Glueballs, hybrid and exotic mesons, hep-ph/0101287; C.J. Morningstar, M.J. Peardon, Phys. Rev. D **60**, 034509 (1999)
14. N. Ishii, H. Suganuma, H. Matsufuru, Phys. Rev. D **66**, 094506 (2002)
15. G. Bali et al. (SESAM Coll.), Phys. Rev. D **62**, 054503 (2000); A. Hart, M. Teper, Phys. Rev. D **65**, 034502 (2002)
16. J. Letessier, J. Rafelski, Cambridge Monogr. Part. Phys. Nucl. Cosmol. **18**, 1 (2002), and references therein

17. F. Karsch, E. Laermann, A. Peikert, Nucl. Phys. B **605**, 579 (2001)
18. T. DeGrand, R.L. Jaffe, K. Johnson, J. Kiskis, Phys. Rev. D **15**, 2060 (1975)
19. C. Bernard et al., Phys. Rev. D **56**, 5584 (1997) and references therein
20. A. Ali Khan et al. (CP-PACS Coll.), Phys. Rev. D **63**, 034502 (2001)
21. R.G. Edwards, U.M. Heller, Phys. Lett. B **462**, 132 (1999)
22. A. Peikert, QCD thermodynamics with 2+1 quark flavours in lattice simulations, Ph.D. thesis, University of Bielefeld (2000)
23. S. Aoki et al. (CP-PACS Coll.), Phys. Rev. D **67**, 034503 (2003)
24. LHPC Collaboration: D.G. Richards, QCDSF Collaboration: M. Göckeler, R. Horsley, D. Pleiter, P.E.L. Rakow, G. Schierholz, UKQCD Collaboration: C.M. Maynard, Nucl. Phys. Proc. Suppl. **109**, 89 (2002)
25. F.X. Lee, D.B. Leinweber, Phys. Rev. D **59**, 074505 (1999)
26. F. Karsch, E. Laermann, A. Peikert, Phys. Lett. B **478**, 447 (2000)
27. For a recent compilation of data see for instance: F. Karsch, E. Laermann, Thermodynamics and in-medium hadron properties from lattice QCD, to appear in Quark Gluon Plasma 3, edited by R. Hwa, X.-N. Wang
28. F. Karsch, Nucl. Phys. A **698**, 199c (2002)
29. R.D. Pisarski, O. Alvarez, Phys. Rev. D **26**, 3735 (1982)